JSHC
Japan Society of Histochemistry and Cytochemistry
Established 1959

Acta Histochem. Cytochem. 45 (2): 139–146, 2012
doi:10.1267/ahc.12003

Close Association of Aquaporin-2 Internalization with Caveolin-1

Takeo Aoki[1], Takeshi Suzuki[1], Haruo Hagiwara[1,4], Michio Kuwahara[2], Sei Sasaki[3], Kuniaki Takata[1] and Toshiyuki Matsuzaki[1]

[1]Department of Anatomy and Cell Biology, Gunma University Graduate School of Medicine, Maebashi, Gunma 371–8511, Japan, [2]Division of Nephrology, Shuwa General Hospital, Kasukabe Saitama 344–0035, Japan, [3]Department of Nephrology, Tokyo Medical and Dental University Graduate School, Tokyo 113–8519, Japan and [4]Present address: Department of Anatomy, Teikyo University School of Medicine, Tokyo 173–8605, Japan

Received January 26, 2012; accepted February 15, 2012; published online April 21, 2012

Aquaporin 2 (AQP2) is a membrane water channel protein that traffics between the intracellular membrane compartment and the plasma membrane in a vasopressin-dependent manner in the renal collecting duct cell to control the amount of water reabsorption. We examined the relation between AQP2 internalization from the plasma membrane and caveolin-1, which is a major protein in membrane microdomain caveolae, in Mardin-Darby canine kidney cells expressing human AQP2 (MDCK-hAQP2 cells). Double-immunofluorescence microscopy showed that AQP2 is colocalized with caveolin-1 in the apical plasma membrane by stimulating the intracellular signaling cascade of vasopressin with forskolin. After washing forskolin, both AQP2 and caveolin-1 were internalized to early endosomes and then separately went back to their individual compartments, which are subapical compartments and the apical membrane, respectively.

Double-immunogold electron microscopy in ultrathin cryosections confirmed the colocalization of AQP2 with caveolin-1 at caveolar structures on the apical plasma membrane of forskolin-treated cells and the colocalization within the same intracellular vesicles after washing forskolin. A co-immunoprecipitation experiment showed the close interaction between AQP2 and caveolin-1 in forskolin-treated cells and in cells after washing forskolin. These results suggest that a caveolin-1-dependent and possibly caveolar-dependent pathway is a candidate for AQP2 internalization in MDCK cells.

Key words: aquaporin-2, early endosome, caveolin-1, apical membrane, MDCK cells

I. Introduction

Water transfer through the plasma membrane lipid bilayer is markedly increased by membrane water channel proteins, aquaporins. So far, 13 aquaporin isoforms have been identified in mammals and their tissue distributions are becoming clear [10, 11]. In the kidney, at least 7 isoforms, aquaporin-1 (AQP1), AQP2, AQP3, AQP4, AQP6, AQP7, and AQP11, are expressed in specific cell membrane domains (for review, see [26, 27]). AQP2 is an important water channel in the collecting duct principal cells, where it is largely distributed in the apical region. It is well known that AQP2 traffics between intracellular vesicles and the plasma membrane by exocytotic membrane insertion and endocytotic internalization (for review, see [4, 27, 28]). When the plasma vasopressin level is high, exocytotic membrane insertion of AQP2 is accelerated and AQP2 is much accumulated on the apical membrane, which mediates rapid and efficient transfer of water from the lumen into the cell. AQP3 and AQP4 are localized on the basolateral membrane of these cells, leading water to the interstitium. These aquaporins in concert mediate water reabsorption and urinary concentration. When the plasma vasopressin

Correspondence to: Takeo Aoki, Ph.D, Department of Anatomy and Cell Biology, Gunma University Graduate School of Medicine, 3–39–22 Showa-machi, Maebashi, Gunma 371–8511, Japan.
E-mail: aoki-take@gunma-u.ac.jp

level falls, AQP2 on the apical membrane is internalized to intracellular vesicles by endocytosis. AQP2 is internalized to the early endosome compartment and some is recycled back to the subapical recycling compartment in Madin-Darby canine kidney cells, which stably express human AQP2 (MDCK-hAQP2 cells; [24, 25]). Recently, we became interested in the relationship between AQP2 internalization and plasma membrane microdomains, which are specific domains where specific types of lipids, such as cholesterol and sphingolipids, are concentrated. Caveolae are caveolin-1-enriched flask-shaped 60–80 nm invaginations of the plasma membrane that form a subdomain of microdomains (for review, see [9, 15, 17]). Caveolin-1 forms high molecular mass oligomers, which likely facilitate, but are not sufficient for, the formation of the caveolar structure (for review, see [9]). The functions of caveolae are diverse and include endocytosis, transcytosis, potocytosis, calcium signaling, and the regulation of various signaling events (for review, see [15]). It is well known that caveolae offer an endocytotic pathway to viruses such as influenza [13] and Simian virus 40 (SV40; [16]), as well as membrane proteins such as sugar transporter GLUT4 [18], occludin [19], and claudin-5 [19]. Whether caveolae are involved in the trafficking of AQP2 has not been documented. In the present study we examined the interaction between AQP2 and a major caveolar protein, caveolin-1, in the course of AQP2 trafficking in MDCK-hAQP2 cells.

II. Materials and Methods

Cell culture

Madin-Darby canine kidney (MDCK) cells, which stably express human AQP2 (MDCK-hAQP2), were used [3, 6, 24, 25]. Cells were maintained in Dulbecco's modified Eagle's medium (DMEM) supplemented with 10% fetal bovine serum (FBS), 100 U/ml penicillin, 100 μg/ml streptomycin, and 250 μg/ml G418, at 37°C with 5% CO_2. For analyses, cells were seeded onto permeable supports (Transwell; Costar, Cambridge, MA), glass coverslips, or directly onto plastic dishes and grown as confluent monolayers. To induce AQP2 trafficking to the plasma membrane, cells were treated with 50 μM forskolin (Sigma, St. Louis, MO) in DMEM-10% FBS for 30 min. Internalization of AQP2 was induced by incubation of cells in DMEM-10% FBS without forskolin for 30, 60, 90, or 120 min at 37°C with 5% CO_2 after complete washout with 30 ml DMEM-10% FBS without forskolin.

Co-transfection

Plasmid containing cDNA for flotillin-2 fused in the N-terminus of EGFP (flotillin-2-EGFP) was kindly provided by Dr. R Tikkanen [12]. Flotillin-2-EGFP was transiently expressed in MDCK-hAQP2 cells by transfection using Lipofectamine 2000 (Invitrogen, Carlsbad, CA).

Antibodies

Primary antibodies were as follows: rabbit anti-AQP2 [23, 24], guinea pig anti-AQP2 [23, 24], goat anti-AQP2 (sc-9882; Santa Cruz Biotechnology, Santa Cruz, CA), rabbit anti-Rab11a (Zymed, San Francisco, CA), mouse anti-EEA1 (clone 14; BD Biosciences, San Jose, CA), goat anti-EEA1 (sc-6414, Santa Cruz Biotechnology), mouse anti-caveolin-1 (clone 2234, BD Biosciences), rabbit anti-caveolin-1 (sc-894, Santa Cruz Biotechnology), mouse anti-phosphorylated caveolin-1 (clone 56, BD Biosciences), rabbit anti-cathepsin D [8], and mouse anti-gp135 [14]. Secondary antibodies were as follows: Alexa Fluor 488-conjugated donkey anti-rabbit, anti-mouse, or anti-goat IgG antibodies (Molecular Probes, Eugene, OR), Rhodamine Red X-conjugated donkey anti-mouse, anti-rabbit, or anti-goat IgG antibodies (Jackson ImmunoResearch, West Grove, PA).

Immunocytochemistry

Cells were seeded onto either permeable supports (Transwell, Costar) or glass coverslips and grown as confluent monolayers. After various treatments, cells were fixed with 2% paraformaldehyde in 0.1 M phosphate buffer (pH 7.4) for 30 min at room temperature, methanol for 10 min on ice, or acetone for 10 min on ice. Cells on permeable supports were then sectioned perpendicular to the filters with a cryostat and mounted on MAS-coated glass slides (Matsunami, Osaka, Japan). Cells on glass coverslips fixed with paraformaldehyde solution were treated with 0.1% Triton X-100 in phosphate-buffered saline (PBS) for 20 min and then processed for immunostaining. To prevent non-specific binding of antibodies, cells were treated with either 3% bovine serum albumin (BSA) in PBS or 2% gelatin in PBS and then sequentially incubated with the primary and secondary antibodies. Nuclei were stained with either 4',6-diamidino-2-phenylindole (DAPI) or TO-PRO-3 (Invitrogen). Specimens were mounted with mounting medium including 1,4-diazabicyclo(2,2,2)octane and observed with an Axioplan 2 microscope equipped with a MRC-1024ES laser confocal system (Carl Zeiss, Jena, Germany), or an IX81 microscope equipped with a FV1000 laser confocal system (Olympus, Tokyo, Japan). Digital images were processed with Photoshop CS5 software (Adobe, San Jose, CA).

Immunoelectron microscopy

Cells were fixed with 3% paraformaldehyde in 0.1 M sodium phosphate buffer (pH 7.4) for 30 min, scraped and embedded in 10% agarose. Cells were then infiltrated with a mixture of sucrose–polyvinyl pyrrolidone and frozen rapidly in liquid nitrogen [29]. Ultrathin cryosections were cut using a Leica Ultracut S equipped with an FCS cryosectioning system (Leica Microsystems, Vienna, Austria) using a cryodiamond knife. Indirect immunogold staining of ultrathin cryosections was performed essentially as described previously [7]. Sections were picked up with a mixture of 2.3 M sucrose and 2% methylcellulose (0.025 Pa·s), and were transferred to Formvar (Oken-shoji, Tokyo, Japan) and carbon-coated copper grids. Immunostaining was performed by floating the grids on drops of diluted

antibodies. Non-specific binding was blocked by pretreatment with 3% BSA in PBS for 10 min. In the double-staining procedure, sections were first incubated with a mixture of primary antibodies raised in different animal species and then with a mixture of species-specific secondary antibodies conjugated with 6- or 12-nm colloidal gold (Jackson ImmunoResearch). Specimens were washed with 0.1% BSA in PBS and then with PBS without BSA. These sections were fixed with glutaraldehyde and ultrathin-embedded in a mixture of 0.2% uranyl acetate and 2% methylcellulose at 4°C. Specimens were dried and observed with a JEM-100CX electron microscope (JEOL, Tokyo, Japan).

Preparation of Triton X-100-soluble and -insoluble fractions

Cells were grown in the culture dishes. After various treatments, cells were incubated with ice-cold 25 mM 2-(N-morpholino) ethanesulfonic acid (MES) buffer, pH 6.5, containing 1% Triton X-100, 150 mM NaCl, 1 mM (p-amidinophenyl) methanesulfonyl fluoride (APMSF) for 30 min on ice. Cells were then scraped, passed through a 26-gauge syringe and centrifuged at 15,000 rpm for 10 min at 4°C. The supernatant and pellet were collected as Triton X-100-soluble and -insoluble fractions, respectively. Triton X-100-soluble proteins were precipitated with 10% trichloroacetic acid or acetone. They were then subjected to sodium dodecyl sulfate-acrylamide gel electrophoresis (SDS-PAGE) and immunoblot analysis.

Co-immunoprecipitaion procedure

Cells were grown in the culture dishes. After various treatments, cells were incubated with ice-cold Tris-HCl buffer, pH 7.5, containing 1% Triton X-100, 150 mM EDTA, 60 mM n-octyl-beta-D-glucoside, 1 mM APMSF, 2 mg/ml leupeptin, and 2 mg/ml pepstatin A for 30 min on ice. Cells were then scraped, passed through a 26-gauge syringe and centrifuged at 15,000 rpm for 10 min at 4°C to remove cell debris. The supernatant was sequentially incubated with primary antibodies against AQP2 or caveolin-1 and secondary antibodies and then precipitated with agarose beads prebound to protein A or protein G (Santa Cruz Biotechnology). Co-immunoprecipitation samples were then subjected to SDS-PAGE and immunoblot analysis.

SDS-PAGE and immunoblot analysis

Samples were denatured in the buffer (15 mM Tris-HCl, pH 8.0, containing 20% sucrose, 2.5% SDS, and 5% 2-mercapto-ethanol) by boiling for 5 min, separated on 15% SDS-PAGE, and then electrotransferred to nitrocellulose membranes (Hybond; GE Healthcare/Amersham, Buckinghamshire, UK). The blots were sequentially incubated with primary antibodies and horseradish peroxidase-conjugated secondary antibodies. Signals were visualized on Hyperfilm ECL (GE Healthcare/Amersham) using chemiluminescence (Supersignal West Dura Extended Duration Substrate; Pierce, Rockford, IL).

III. Results

Immunofluorescence microscopy of AQP2 and caveolin-1 in MDCK cells

Since MDCK-hAQP2 cells do not express vasopressin receptor, forskolin was used to increase cAMP, which is a second messenger of the intracellular cascade. Figure 1 shows the changes of AQP2 distribution upon forskolin treatment and subsequent wash out of forskolin in polarized MDCK-hAQP2 cells. Compared to the immunofluorescence of an apical membrane marker, Gp135, AQP2 was localized largely in the subapical cytoplasm and slightly on the apical membrane. Upon treatment with forskolin for 30 min, AQP2 appeared largely on the apical membrane by exocytosis. After washing and incubation without forskolin for 30 min, AQP2 was internalized in the cytoplasm by endocytosis. These results are in accord with our previous studies [24]. Then we examined the changes of the distribution of AQP2 and caveolin-1 during exocytosis and endocytosis by double-immunofluorescence microscopy (Fig. 2). In the control state, AQP2 was largely found in the subapical cytoplasm, as shown in Figure 1, and caveolin-1 was seen largely in the apical membrane and slightly in the cytoplasm. Upon treatment with forskolin, AQP2 and caveolin-1 were colocalized on the apical membrane (Fig. 2d–f). After washing and incubation without forskolin for 30 min, both AQP2 and caveolin-1 were internalized and partially colocalized in the cytoplasm, forming vesicle-like structures (Fig. 2g–i). Colocalization of AQP2 and caveolin-1 in the cytoplasm was seen up to 90 min after washing (data not shown).

Co-immunoprecipitation of AQP2 and caveolin-1

It is well known that caveolin-1 is a Triton X-100-insoluble protein [2]. To examine whether AQP2 is recovered in the Triton X-100-insoluble fraction, we performed immunoblotting of Triton X-100-soluble and -insoluble fractions from MDCK-hAQP2 cell lysates. Both caveolin-1 and AQP2 were almost entirely restricted to the Triton X-100-insoluble fraction (Fig. 3). To reveal the interaction of AQP2 and caveolin-1, we performed co-immunoprecipitation using anti-AQP2 antibody and anti-caveolin-1 antibody. Figure 4a shows that anti-AQP2 antibody was able to co-immunoprecipitate caveolin-1 to a higher degree from forskolin-treated cell lysate, but very faintly from control cell lysate. A positive band for caveolin-1 around 22–24 kDa was confirmed by the results of immunoprecipitation using anti-caveolin-1 antibody. Two additional bands around 20 and 40 kDa seemed to be rabbit anti-AQP2 antibody detected by HRP-labeled goat anti-rabbit IgG antibody, since these bands were also detected in the lane in which normal rabbit IgG was electrophoresed. Figure 4b shows that cavevolin-1 was still co-immunoprecipitated with AQP2 after washing out forskolin. We previously showed that internalized caveolin-1 was phosphorylated using phosphorylated caveolin-1-specific antibody [1]. To test whether caveolin-1 is phosphorylated

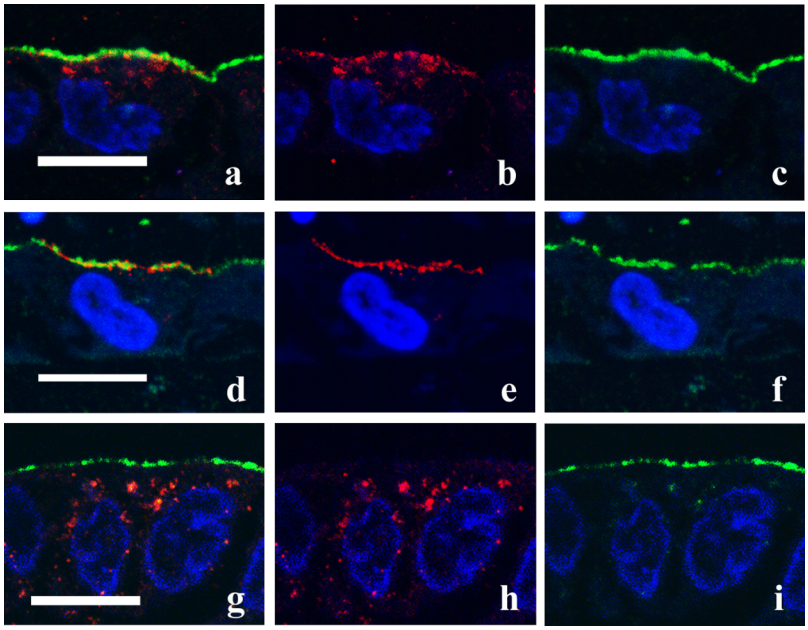

Fig. 1. Trafficking of AQP2 in MDCK-hAQP2 cells. Confluent MDCK-hAQP2 cells grown on permeable supports without any treatment as a control (**a–c**), treated with forskolin for 30 min (**d–f**), or treated with forskolin for 30 min, washed, and then incubated without forskolin for 30 min (**g–i**) were fixed. Cells were sectioned perpendicular to the permeable support with a cryostat and double-immunofluorescently labeled for AQP2 (red) and the apical membrane marker Gp135 (green). Nuclei were stained with DAPI (blue). Merged confocal images are shown on the left. AQP2 is largely seen in the subapical cytoplasm in the control. Upon forskolin treatment, AQP2 is accumulated on the apical membrane. AQP2 is internalized and seen in the cytoplasm after washing out forskolin. Bar=10 μm.

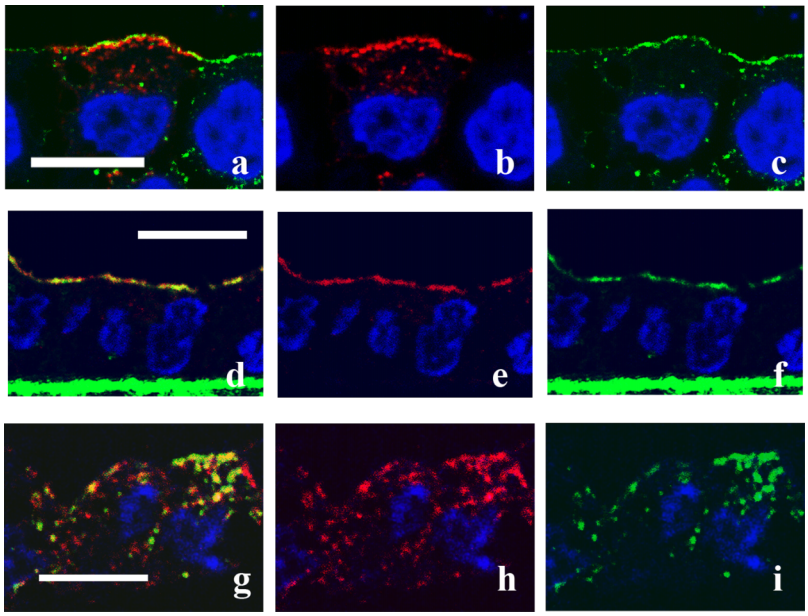

Fig. 2. Colocalization of AQP2 and caveolin-1. Confluent MDCK-hAQP2 cells grown on permeable supports without any treatment as a control (**a–c**), treated with forskolin for 30 min (**d–f**), or treated with forskolin for 30 min, washed, and then incubated without forskolin for 30 min (**g–i**) were fixed. Cells were sectioned perpendicular to the supports with a cryostat and double-immunofluorescently labeled for AQP2 (red) and caveolin-1 (green). Nuclei were stained with DAPI (blue). Merged confocal images are shown on the left. In the control, AQP2 is seen in the subapical cytoplasm and seems not to colocalize with caveolin-1, which is present on the apical membrane. AQP2 is largely colocalized with caveolin-1 on the apical membrane upon forskolin treatment. Some AQP2 internalized after washout is colocalized with caveolin-1. Bar=10 μm.

when it is internalized after forskolin stimulation, we immunoblotted the cell lysate with phosphorylated caveolin-1-specific antibody. It was found that phosphorylated caveolin-1 was markedly increased after washing out forskolin (Fig. 5).

AQP2 recycling and caveolin-1

We followed the change of AQP2 and caveolin-1 distribution by double-immunofluorescence microscopy after forskolin treatment and the subsequent washing step. Figure 6a–c shows that AQP2 was internalized initially to the EEA1-positive early endosome and then to the subapical compartment 2 hours after washing out forskolin, confirming our previous study [24]. In comparison, Fig. 6d–f shows that caveolin-1, which was colocalized with AQP2 on the apical membrane upon treatment with forskolin, was internalized with AQP2 as far as the EEA1-positive endosome and then returned to the apical membrane 2 hours after washing.

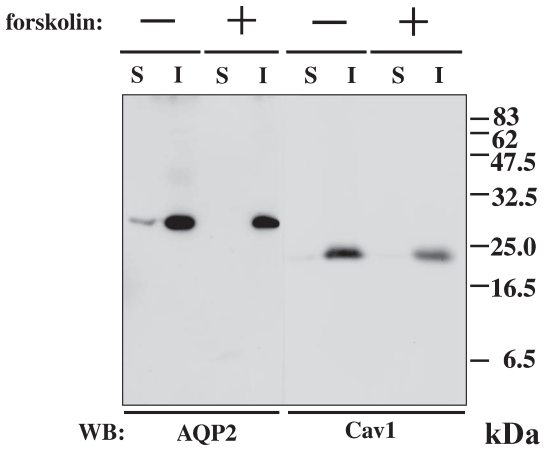

Fig. 3. AQP2 is recovered in Triton X-100-insoluble fraction. Samples of Triton X-100-soluble (S) and -insoluble (I) fractions from MDCK-hAQP2 cell lysates with (+) or without (–) forskolin treatment for 30 min were subjected to SDS-PAGE and immunoblotting using anti-AQP2 and anti-caveolin-1 (Cav1) antibodies.

Immunoelectron microscopy of AQP2 and caveolin-1

To examine the ultrastructural co-localization of AQP2 and caveolin-1, we performed double-immunogold labeling in ultrathin cryosections. Some AQP2 labeling was colocalized with caveolin-1 at caveolar structures on the apical plasma membrane, although some AQP2 was found solely on the microvillous membrane upon treatment with forskolin (Fig. 7a). Co-localization of AQP2 and caveolin-1 labeling within the same intracellular vesicles, sometimes in large vesicles such as multivesicular bodies, was clearly seen 30 min after washing forskolin (Fig. 7b).

AQP2 and flotillin-2

Flotillin-2 is also a membrane microdomain protein that resides in noncaveolar plasma membrane microdomains [20, 21]. To test the relation between AQP2 internalization and flotillin-2, MDCK-hAQP2 cells were transiently transfected with EGFP-tagged flotillin-2 and subjected to forskolin treatment and forskolin washing. AQP2 appeared to colocalize with EGFP-tagged flotillin-2 on the apical membrane 30 min after forskolin treatment (Fig. 6g) and

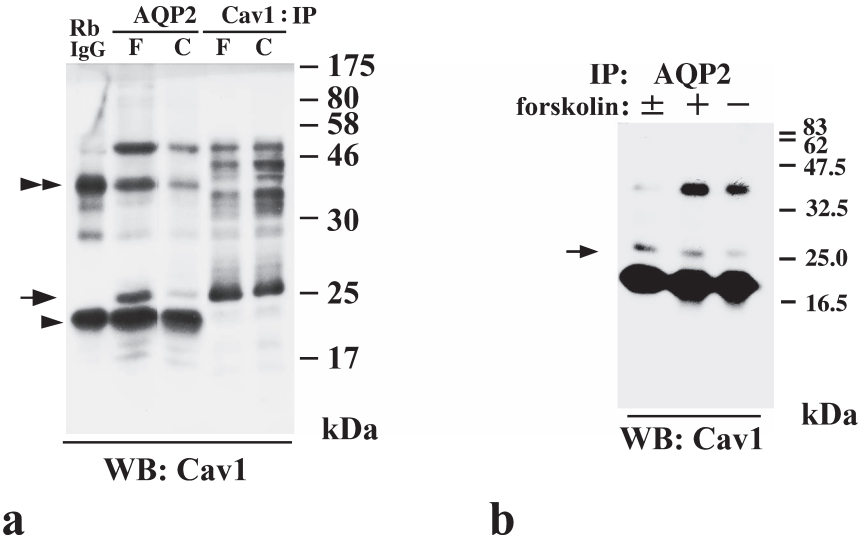

Fig. 4. AQP2 co-immunoprecipitates with caveolin-1. **a**: In immunoprecipitates with anti-AQP2, caveolin-1 is detected as a dense band in forskolin-treated cells (F) and a faint band in control cells (C) at 22–24 kDa (arrow) with anti-caveolin-1 (Cav1). Dense bands both around 20 kDa (arrowhead) and 40 kDa (double-arrowhead) seem to be non-specific because these bands are also detected in the lane in which rabbit IgG was electrophoresed (RbIgG). **b**: Immunoprecipitates with anti-AQP2 from each cell lysate described as follows were subjected to immunoblotting with anti-caveolin-1 (Cav1). –: control cells, +: cells treated with forskolin for 30 min, ±: cells treated with forskolin for 30 min, washed, and then incubated without forskolin for 30 min.

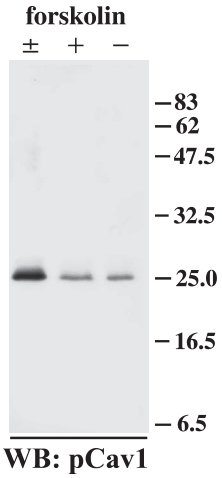

Fig. 5. Internalized caveolin-1 is phosphorylated. Samples of Triton X-100-insoluble fractions from MDCK-hAQP2 cell lysates were subjected to SDS-PAGE and immunoblotting using anti-phosphorylated caveolin-1 antibody. A strong band is detected in cells treated with forskolin and subsequently washed and incubated without forskolin for 30 min (±). Faint bands are detected in cells both treated (+) and untreated (–) with forskolin.

then both appeared to be internalized to the same compartment 30 min after washing (Fig. 6h).

IV. Discussion

AQP2 endocytosis in cultured cell system

The intracellular distribution of AQP2 is controlled by exocytosis and endocytosis. The exocytotic pathway of AQP2 vesicles and its mechanism has been well studied compared to its endocytotic pathway. We focused on the endocytotic and recycling pathways of AQP2 in the present work. We have previously shown that AQP2 on the apical membrane is internalized to EEA1-positive early endosomes, and then recycled back to the subapical storage compartment via the phosphatidylinositol 3-kinase-dependent pathway in MDCK-hAQP2 cells [24]. This *in vitro* study appears to represent the basic nature of AQP2 *in vivo* [23]. There remain some questions regarding the internalization of AQP2 from the apical membrane as performed this study. Sun *et al.* [22] have shown that AQP2 is concentrated in clathrin-coated pits on the surface membrane of AQP2-transfected LLC-PK1 cells. In addition, they demonstrated that AQP2 cycles between the plasma membrane and intracellular vesicles via a dynamin-dependent endocytotic pathway [22]. We show here the possible caveolin-1-dependent AQP2 endocytotic pathway in MDCK-hAQP2 cells. To our knowledge this is the first paper to report the interaction of AQP2 and caveolin-1 along their endocytotic pathway. In addition, as shown in Fig. 7a, caveolar structures were positive for both caveolin-1 and AQP2. Taken together, our results suggest that the caveolin-1-dependent pathway, which could also be caveolar de-

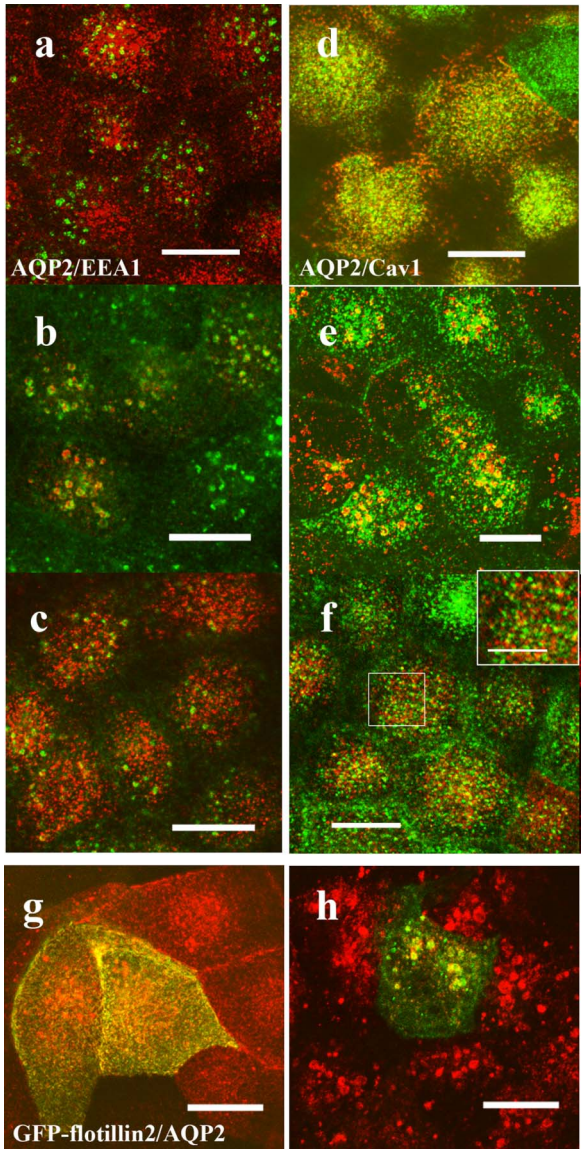

Fig. 6. AQP2 is internalized to the same compartment with caveolin-1 and flotillin-2. (**a–f**) MDCK-hAQP2 cells were seeded on coverslips and subjected to forskolin treatment for 30 min (**a, d**) and subsequent washing and incubation without forskolin for 30 min (**b, e**) or for 2 hr (**c, f**). Double-immunofluorescence labeling for AQP2 and EEA1 (**a–c**) or for AQP2 and caveolin-1 (**d–f**) was carried out and their localization was observed with a laser confocal microscope. Projection images of 4 consecutive confocal images (0.4 μm intervals) are shown. AQP2 is shown in red. EEA1 and caveolin-1 are shown in green. An enlarged view of the rectangle area is shown in the inset (**f**). Both AQP2 and caveolin-1 are internalized in the EEA1-positive compartment 30 min after washing and then differentially localized at 2 hr. **g, h**: MDCK-hAQP2 cells transiently transfected with EGFP-flotillin-2 were treated with forskolin for 30 min (**g**) and then washed and incubated without forskolin for 30 min (**h**). Localization of AQP2 and flotillin-2 was observed with a laser confocal microscope. Projection images of 4 consecutive confocal images (0.4 μm intervals) are shown. AQP2 is shown in red. EGFP fluorescence is shown in green. Both AQP2 and EGFP-flotillin-2 are internalized in the same compartment. Bars=10 μm (5 μm in inset).

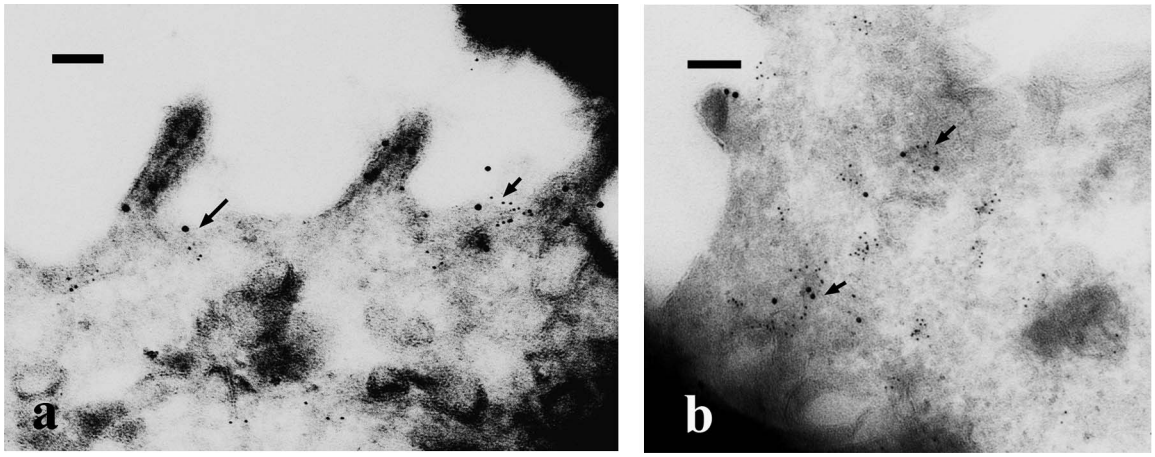

Fig. 7. Ultrastructural localization of AQP2 and caveolin-1. MDCK-hAQP2 cells were treated with forskolin for 30 min (**a**), and then washed and incubated without forskolin for 30 min (**b**). Ultrathin cryosections were double-labeled for AQP2 (12 nm colloidal gold) and caveolin-1 (6 nm colloidal gold). In forskolin-treated cells (**a**), some AQP2 is colocalized with caveolin-1 at caveolar structures in the apical membrane domain (arrows). AQP2 on the microvillous membrane is not colocalized with caveolin-1. When cells were washed and incubated without forskolin for 30 min (**b**), AQP2 was colocalized with caveolin-1 in the intracellular vesicles (arrows). Bars=100 nm.

pendent, is a candidate for AQP2 internalization, at least in MDCK cells. Co-immunoprecipitation analysis showed the close interaction between AQP2 and caveolin-1 in an early step of the endocytotic pathway. Caveolin-1 might have direct or indirect roles in inducing AQP2 to endosomes in MDCK-hAQP2 cells. Since AQP2 was internalized with flotillin-2 as well as caveolin-1, AQP2 internalization appears to be related with at least some membrane microdomains. We examined whether AQP2 is internalized by the clathrin-dependent pathway as well in MDCK-hAQP2 cells. Apparent co-localization of AQP2 and clathrin heavy chain was not seen when double-immunofluorescence labeling was performed after washing forskolin (data not shown). Of course our results do not exclude the possibility of clathrin-dependent internalization of AQP2. As in the case of influenza virus, which may be internalized via caveolae in addition to entry by clathrin-mediated endocytosis [13], AQP2 might be internalized via both microdomain-dependent and clathrin-dependent pathways.

Comparison with in vivo studies

We showed here that AQP2 is internalized with caveolin-1 in MDCK cells. In comparison, it is thought that AQP2 is probably internalized via the clathrin-mediated pathway in the renal collecting duct cells because AQP2 was found to be localized in clathrin-coated pits in these cells [22]; therefore, we have to carefully discuss the possibility of caveolin-1- and caveolar-dependent AQP2 internalization in the renal collecting duct cells.

In accordance with our results in MDCK cells, reports regarding the relation between AQP2 and membrane microdomain have recently been seen in renal collecting duct cells. Feng *et al.* [5] revealed that AQP2 is nearly evenly distributed in caveolin-1-positive lipid raft fractions and non-raft fractions in isolated kidney inner medullary collecting duct cells. Interestingly, Yu *et al.* [30] demonstrated that serine 256-phosphorylated AQP2 is greater in the detergent-resistant membrane fraction than in the non-detergent-resistant membrane fraction. Together with our *in vitro* study, it may be safe to say that AQP2 internalization can occur in some instances via membrane microdomain-related pathways in addition to the clathrin-mediated pathway. Further studies would help to clarify these points.

V. Acknowledgments

We thank Y. Takahashi-Tajika and M. Shimoda for their assistance. This work was supported in part by Grants-in-Aid for Scientific Research from the Ministry of Education, Culture, Sports, Science, and Technology of Japan.

VI. References

1. Aoki, T., Nomura, R. and Fujimoto, T. (1999) Tyrosine phosphorylation of caveolin-1 in the endothelium. *Exp. Cell Res.* 253; 629–636.
2. Aoki, T., Hagiwara, H., Matsuzaki, T., Suzuki, T. and Takata, K. (2007) Internalization of caveolae and their relationship with endosomes in cultured human and mouse endothelial cells. *Anat. Sci. Int.* 82; 82–97.
3. Asai, T., Kuwahara, M., Kurihara, H., Sakai, T., Terada, Y., Marumo, F. and Sasaki, S. (2003) Pathogenesis of nephrogenic diabetes insipidus by aquaporin-2 C-terminus mutations. *Kidney Int.* 64; 2–10.
4. Brown, D. (2003) The ins and outs of aquaporin-2 trafficking. *Am. J. Physiol. Renal. Physiol.* 284; F893–F901.
5. Feng, X., Huang, H., Yang, Y., Frohlich, O., Klein, J. D., Sands, J. M. and Chen, G. (2009) Caveolin-1 directly interacts with UT-A1 urea transporter: the role of caveolae/lipid rafts in UT-A1 regulation at the cell membrane. *Am. J. Physiol. Renal Physiol.* 296; F1514–F1520.
6. Hasegawa, T., Matsuzaki, T., Tajika, Y., Ablimit, A., Suzuki, T.,

Aoki, T., Hagiwara, H. and Takata, K. (2007) Differential localization of aquaporin-2 and glucose transporter 4 in polarized MDCK cells. *Histochem. Cell Biol.* 127; 233–241.
7. Heijnen, H. F. G., Debili, N., Vainchencker, W., Breton-Gorius, J., Geuze, H. J. and Sixma, J. J. (1998) Multivesicular bodies are an intermediate stage in the formation of platelet alpha-granules. *Blood* 91; 2313–2325.
8. Kominami, E., Bando, Y., Wakamatsu, N. and Katunuma, N. (1984) Different tissue distributions of two types of thiol proteinase inhibitors from rat liver and epidermis. *J. Biochem.* 96; 1437–1442.
9. Lajoie, P. and Nabi, I. R. (2010) Lipid rafts, caveolae, and their endocytosis. *Int. Rev. Cell Mol. Biol.* 282; 135–163.
10. Matsuzaki, T., Hata, H., Ozawa, H. and Takata, K. (2009) Immunohistochemical localization of the aquaporins AQP1, AQP3, AQP4, and AQP5 in the mouse respiratory system. *Acta Histochem. Cytochem.* 42; 159–169.
11. Matsuzaki, T., Inahata, Y., Sawai, N., Yang, C.-Y., Kobayashi, M., Takata, K. and Ozawa, H. (2011) Immunohistochemical localization of the water channels AQP4 and AQP5 in the rat pituitary gland. *Acta Histochem. Cytochem.* 44; 259–266.
12. Neumann-Giesen, C., Falkenbach, B., Beicht, P., Claasen, S., Lüers, G., Stuermer, C. A. O., Herzog, V. and Tikkanen, R. (2004) Membrane and raft association of reggie-1/flotillin-2: role of myristoylation, palmitoylation and oligomerization and induction of filopodia by overexpression. *Biochem. J.* 378; 509–518.
13. Nunes-Correia, I., Eulálio, A., Nir, S. and De Lima, M. C. P. (2004) Caveolae as an additional route for influenza virus endocytosis in MDCK cells. *Cell Mol. Biol. Lett.* 9; 47–60.
14. Ojakian, G. K. and Schwimmer, R. (1988) The polarized distribution of an apical cell surface glycoprotein is maintained by interactions with the cytoskeleton of Madin-Darby canine kidney cells. *J. Cell Biol.* 107; 2377–2387.
15. Parton, R. G. and Simons, K. (2007) The multiple faces of caveolae. *Nature Rev. Mol. Cell Biol.* 8; 185–194.
16. Pelkmans, L., Kartenbeck, J. and Helenius, A. (2001) Caveolar endocytosis of simian virus 40 reveals a new two-step vesicular-transport pathway to the ER. *Nature Cell Biol.* 3; 473–483.
17. Pelkmans, L. (2005) Secrets of caveolae- and lipid raft-mediated endocytosis revealed by mammalian viruses. *Biochim. Biophys. Acta* 1746; 295–304.
18. Shigematsu, S., Watson, R. T., Khan, A. H. and Pessin, J. E. (2003) The adipocyte plasma membrane caveolin functional/structural organization is necessary for the efficient endocytosis of GLUT4. *J. Biol. Chem.* 278; 10683–10690.
19. Stamatovic, S. M., Keep, R. F., Wang, M. M., Jankovic, I. and Andjelkovic, A. V. (2009) Caveolae-mediated internalization of occludin and claudin-5 during CCL2-induced tight junction remodeling in brain endothelial cells. *J. Biol. Chem.* 284; 19053–19066.
20. Stuermer, C. A. O., Lang, D. M., Kirsch, F., Wiechers, M., Deininger, S. O. and Plattner, H. (2001) Glycosylphosphatidyl inositol-anchored proteins and fyn kinase assemble in non-caveolar plasma membrane microdomains defined by reggie-1 and -2. *Mol. Biol. Cell* 12; 3031–3045.
21. Stuermer, C. A. O. (2011) Reggie/flotillin and the targeted delivery of cargo. *J. Neurochem.* 116; 708–713.
22. Sun, T. X., Van Hoek, A., Huang, Y., Bouley, R., McLaughlin, M. and Brown, D. (2002) Aquaporin-2 localization in clathrin-coated pits: inhibition of endocytosis by dominant-negative dynamin. *Am. J. Physiol. Renal Physiol.* 282; 998–1011.
23. Tajika, Y., Matsuzaki, T., Suzuki, T., Aoki, T., Hagiwara, H., Tanaka, S., Kominami, E. and Takata, K. (2002) Immunohistochemical characterization of the intracellular pool of water channel aquaporin-2 in the rat kidney. *Anat. Sci. Int.* 77; 189–195.
24. Tajika, Y., Matsuzaki, T., Suzuki, T., Aoki, T., Hagiwara, H., Kuwahara, M., Sasaki, S. and Takata, K. (2004) Aquaporin-2 is retrieved to the apical storage compartment via early endosomes and phosphatidylinositol 3-kinase-dependent pathway. *Endocrinology* 145; 4375–4383.
25. Tajika, Y., Matsuzaki, T., Suzuki, T., Ablimit, A., Aoki, T., Hagiwara, H., Kuwahara, M., Sasaki, S. and Takata, K. (2005) Differential regulation of AQP2 trafficking in endosomes by microtubules and actin filaments. *Histochem. Cell Biol.* 124; 1–12.
26. Takata, K., Matsuzaki, T. and Tajika, Y. (2004) Aquaporins: water channel proteins of the cell membrane. *Prog. Histochem. Cytochem.* 39; 1–83.
27. Takata, K., Matsuzaki, T., Tajika, Y., Ablimit, A., Suzuki, T., Aoki, T. and Hagiwara, H. (2005) Aquaporin water channels in the kidney. *Acta Histochem. Cytochem.* 38; 199–207.
28. Takata, K., Matsuzaki, T., Tajika, Y., Ablimit, A. and Hasegawa, H. (2008) Localization and trafficking of aquaporin 2 in the kidney. *Histochem. Cell Biol.* 130; 197–209.
29. Tokuyasu, K. T. (1986) Application of cryoultramicrotomy to immunocytochemistry. *J. Microsc.* 143; 139–149.
30. Yu, M. J., Pisitkun, T., Wang, G., Aranda, J. F., Gonzales, P. A., Tchapyjnikov, D., Shen, R. F., Alonso, M. A. and Knepper, M. A. (2008) Large-scale quantitative LC-MS/MS analysis of detergent-resistant membrane proteins from rat renal collecting duct. *Am. J. Physiol. Cell Physiol.* 295; C661–C678.